Characterization of Epoxy–Clay Hybrid Composite Prepared by Emulsion Polymerization

DONG CHOO LEE, LEE WOOK JANG

Department of Polymer Science and Engineering, Inha University, Inchon, 402-751, South Korea

ABSTRACT: This article demonstrates the direct intercalation of an epoxy polymer in the interlayer of Na^+–montmorillonite (MMT) by a step type of polymerization in an aqueous emulsion media. The synthesis and the results of structural and thermal characterizations for this hybrid composite are described. Equimolar quantities of bisphenol A and an epoxy prepolymer ($n = 0.2$) in an emulsion media were polymerized in the presence of Na^+–MMT. X-ray diffraction (XRD) data obtained from the acetone-extracted products show that the basal spacing of the MMT is expanded from 0.96 to 1.64 nm. Thermal characterization for the postcured products by TGA and DSC gave evidence of enhanced thermal stabilities. SEM examination of the uncured products revealed that a disordered phase begins to appear with increasing polymer loading. However, the XRD profile supported that an overwhelming fraction of the nanocomposite contains intercalated clay. Also, the possibility of intercalation by the emulsion technique is proposed on the basis of the swelling characteristics of MMT in aqueous media and the sizes of micelles containing a monomer. © 1998 John Wiley & Sons, Inc. J Appl Polym Sci 68: 1997–2005, 1998

Key words: hybrid composite; nanocomposite; emulsion polymerization; epoxy; montmorillonite

INTRODUCTION

In the past decade, there has been increasing interest about the molecular composite derived from the intercalation of organic polymers into smectite clays.[1,2] Undoubtedly, the interest stems from the hybrid properties synergistically derived from the host and guest, particularly the potential mechanical and thermal properties.[3–5]

The lack of affinity, however, between a hydrophilic silicate interlayer and a hydrophobic polymer makes it difficult to obtain this type of molecular composite, and, hence, most of the intercalation processes so far known are limited to the pretreatment of the silicate layer to be swellable with organic molecules by ion exchange between organic onium salts and the interlayer cations of the clay.

In our recent work on a PMMA–clay hybrid composite, it was confirmed that a simple technique of emulsion polymerization can offer a new approach to the synthesis of a nanocomposite. The X-ray diffraction pattern of the PMMA–clay composite showed that the basal spacing (d_{001}) has expanded by 0.58 nm.

This article describes the structure, synthesis, and thermal property of a hybrid epoxy–clay nanocomposite that can be formed by the intercalation of an epoxy polymer into the host clay interlayer by an emulsion polymerization. A physical picture of polymer intercalation by this emulsion

technique is proposed on the basis of the swelling characteristics of clay in an aqueous system and the distribution behavior of micelle sizes containing monomers in an emulsion system.

EXPERIMENTAL

Materials

Clay purification and its Na^+-exchanging processes were followed by the method described previously.[6] An emulsified epoxy prepolymer, prepared by the base-induced condensation of bisphenol A with epichlorohydrine, was supplied by the Kukdo Chemical Co. (Seoul, Korea) The value of n in the polyether formula,
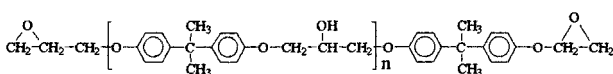
was 0.2 and the molecular mass was 397 g/mol. This emulsified prepolymer has an epoxy functionality of 2, epoxide equivalent weight of 200 $\pm$ 20 g/equiv, and 60 $\pm$ 3 wt % of solid content. A commercial rosin soap, the sodium salt of resin acid, was supplied by the LG Chemical Co. (Seoul, Korea) and employed as a surfactant. The curing agents, dicynodiamin (DICY) and 3-(3,4-dichlorophenyl)-1,1-dimethylurea (DCMU), were also provided by the Kukdo Chemical Co. All the other chemicals used in this work were chemical grades and used without further purification.

Emulsion Polymerization

A heterogeneous reaction between bisphenol A and an emulsified epoxy prepolymer in the presence of Na^+–montmorillonite (MMT) was carried out in a colloidal system with urea. A 2 L three-necked flask was charged with 400 mL of an aqueous dispersion containing 20–80 g of Na^+–MMT. After the system was stirred gently for 1 h at room temperature, 20 mL of the soap solution (solid content: 30 wt %), 200 mL of the emulsified epoxy prepolymer, and an additional 250 mL of water were added. Beginning 3 h later, 100 g of bisphenol A and 5 g of urea in 50 mL of water were introduced. Keeping the stirring rate at 700 rev/min, the reaction was carried out for up to 3 h at 60°C. The polymer latex, so produced, was precipitated by adding 500 mL of an aluminum sulfate solution (17 wt %). The product was separated by filtration, washed intensively, and dried under reduced pressure.

A part of the product was then exposed to hot acetone extraction for up to 5 days, while the remaining part was subjected to postcuring. The curing reaction was carried out by heating 100 g of the unextracted product at 130°C for 1.5 h with 3 g of DCMU and 6 g of DICY, keeping the agitation vigorous. The cured products were pulverized and dried under reduced pressure at 50°C overnight. The experimental difficulty of postcuring the extracted products makes the curing reactions to be limited to the unextracted products.

Characterization and Measurements

Measurement of polymer loading was carried out by thermogravimetric analysis (TGA) using a Du-Pont 9900 thermogravimetric analyzer. A 20 mg mass of the extracted sample was heated to 500°C at a heating rate of 20°C/min under a nitrogen atmosphere. The average molecular masses and the distribution behaviors of the polymers being recovered from the composite extracts were determined by size-exclusion chromatography. A Waters Model 201 equipped with a U6K injector, an M6000A solvent delivery system, and three linear columns packed with μ-Styragel was used. FTIR spectra were recorded on a Nicolet spectrophotometer in the wavenumber range 4000–400 cm^{-1} and the KBr method was used. X-ray diffraction (XRD) patterns of the solid-state samples were obtained from a Philips PW-1847 X-ray crystallographic unit mounted with a Guiniar focusing camera. The CuKα radiation source was operated at 40 kV and 20 mA. Patterns were recorded by monitoring those diffractions that appeared in the 2θ 2°–30° range. Thermal characterizations for the products cured or uncured were carried out by both differential scanning calorimetry (DSC, DuPont 2100 differential scanning calorimeter) and TGA. DSC measurement was carried out by heating 10 mg of the sample to 160°C at a heating rate of 10°C/min under a nitrogen atmosphere, and the data obtained from the second scanning were accepted. The composite microstructure was imaged by an SEM JSM-840A, JEOL, operated with a high-tension voltage of 20 kV.

RESULTS AND DISCUSSION

Polymer-Loading Behavior

The content of the polymer loading was determined by TGA. Thermograms obtained from the
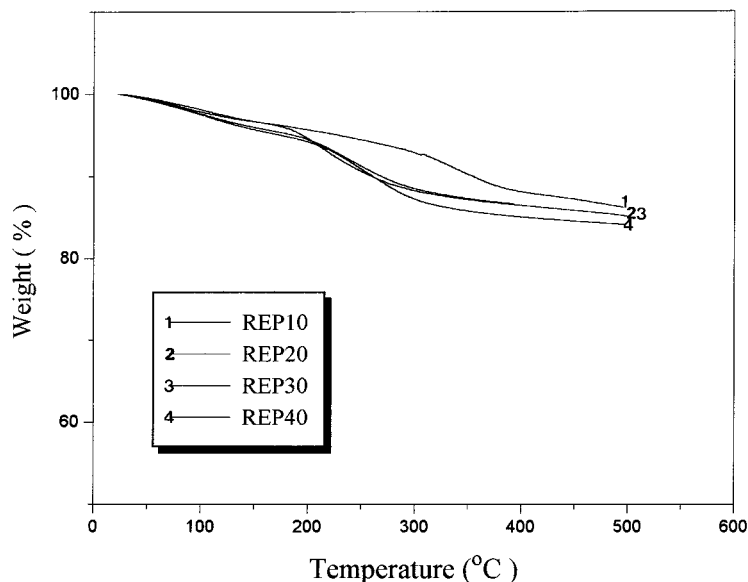
Figure 1   TGA thermograms of the extracted nanocomposites.

extracted products are illustrated in Figure 1. The notation REP in the figure means that the samples are extracted but uncured and the numbers indicate the MMT contents (phr). The overall feature revealed by the thermogram is that considerable amounts of unextractable polymers still remained after 120 h of extraction, which can be regarded as the bound polymer to the interlayer of MMT. The content of organic loading, as Table I shows, reaches about 15 wt % on average but increases slightly with increasing content of MMT. Likewise, the expansions of basal spacing with an increasing content of MMT can be seen from Table I. This gallery expansion approxi-

mately up to 0.7 nm is considered to be a consequence of the intercalation of single or double layers of polymer chains.

Structural Characterization

Additional evidence of intercalation is obtained by the structural characterizations carried out on the structural and morphological change and the crystal modifications of pristine MMT by FTIR, SEM, and XRD. Figure 2 illustrates those spectra obtained from the pure epoxy polymer, unextracted and uncured composite (EP), extracted composite (REP), cured composite (CEP), epoxy

Table I   Input Ratio of Comonomers to MMT, Epoxy Polymer Content, and Variation of Interlayer Distances of the Nanocomposite

| Sample Code	Input Ratio (g/g)		Epoxy Polymer Content (wt %)		Basal Spacing (nm)
	Comonomer	MMT[a]	A[b]	B[b]	
MMT[a]	—	—	—	—	0.96
EP10	100	10	86.16	13.51	1.41
EP20	100	20	80.47	13.88	1.49
EP30	100	30	71.98	15.02	1.54
EP40	100	40	64.62	16.23	1.64

[a] Na^+–montmorillonite.
[b] A: products unpurified by extraction. B: products purified by hot acetone extraction for 120 h.
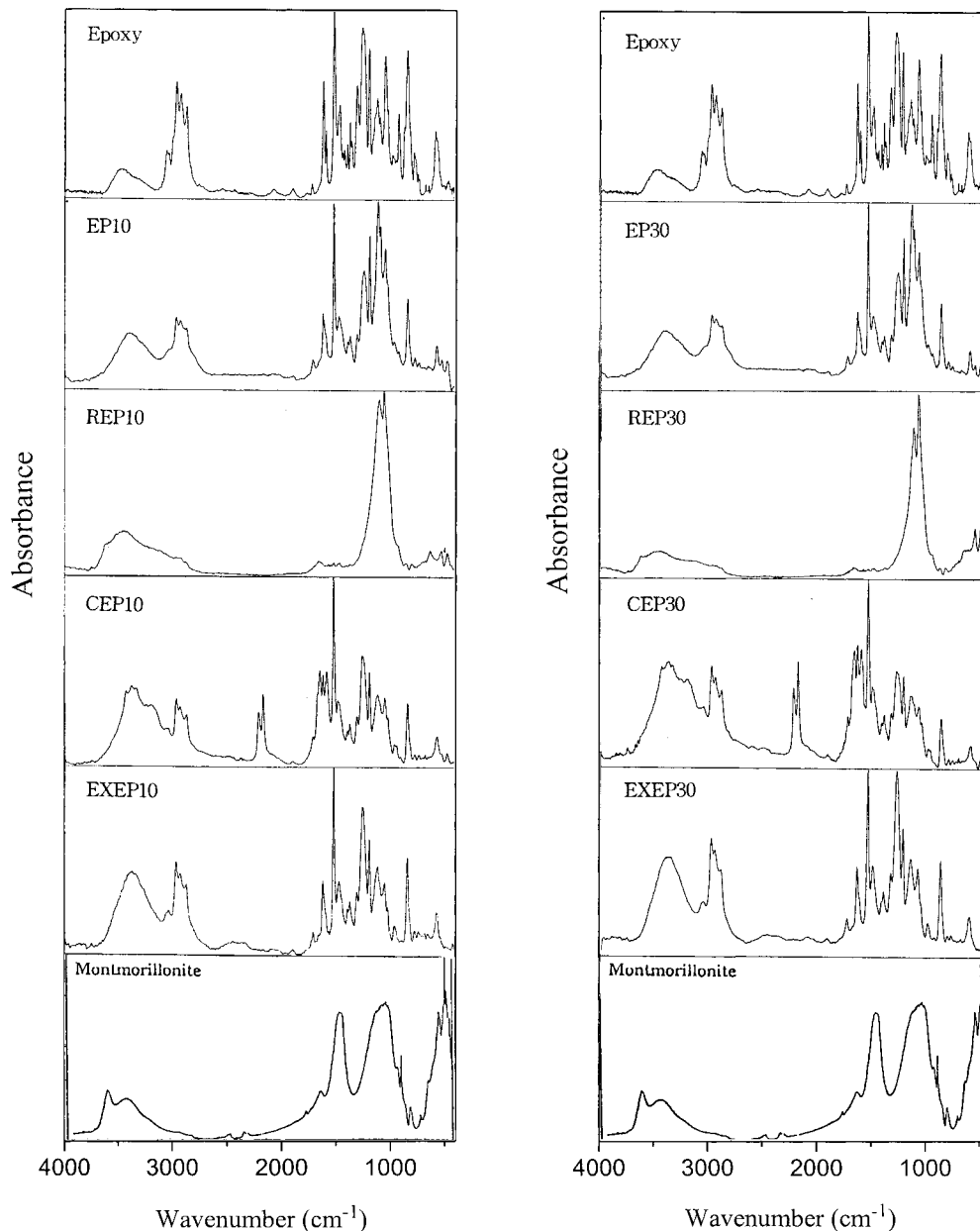
Figure 2   IR spectra of the epoxy homopolymer, MMT, and some of the composites (see the text).

polymer recovered from the composite extracts (EXEP), and the pristine MMT. The spectra of composites either extracted or unextracted reveal the presence of characteristic absorptions of both inorganic and organic components. The peak at 1050 cm^{-1} can be associated with Si—O stretching vibrations, and those that appeared at 3630 cm^{-1} and between 600–400 cm^{-1} can be associated, respectively, with —OH stretching of the

lattice water, Al—O stretching, and Si—O bending. Absorption bands, on the other hand, at 3000–2900 cm^{-1} (CH3 stretching), 1625–1430 cm^{-1} (aromatic C=C stretching), and 950–750 cm^{-1} (epoxide ring vibration) are the consequences of the epoxy polymer. Concurrently, the samples of the CEP series exhibit increasing intensity of the OH band at 3630 cm^{-1} and new bands at 2500–2000 cm^{-1} associated with the cy-
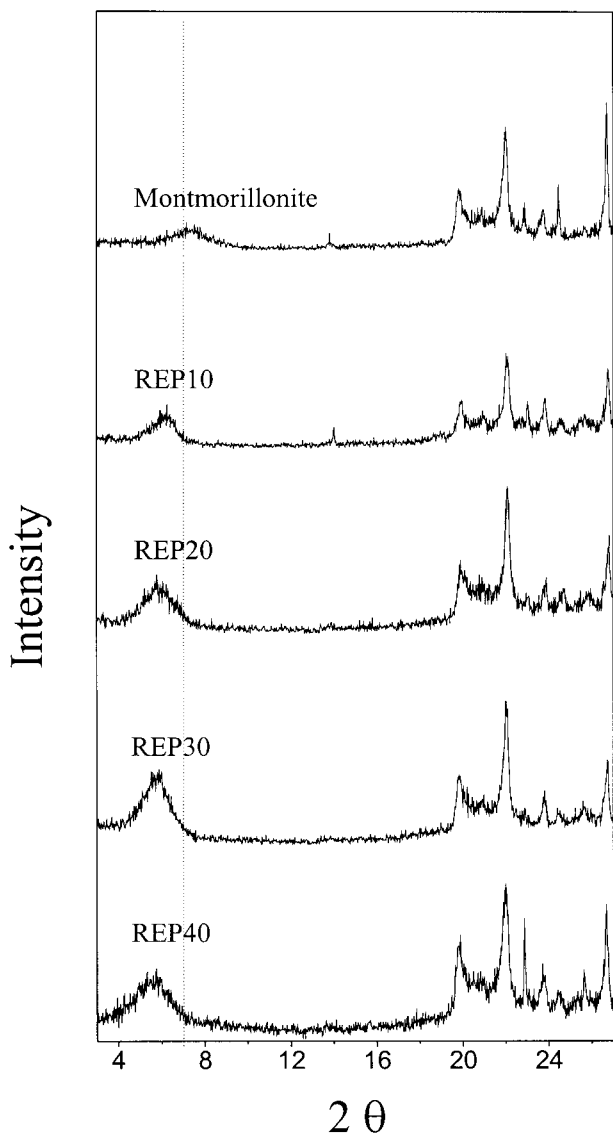
Figure 3 XRD patterns of the extracted nanocomposites and the pure Na^+–MMT.

ano groups which may have resulted from the curing reaction. Nevertheless, no evidence of new bands that could be associated with interactions between organic and inorganic materials was found, suggesting that the fixation of the polymer might have occurred by strong secondary valence forces acting between Na^+ and the polar groups of the epoxy polymer.

Shown in Figure 3 is a series of XRD patterns obtained from the pristine MMT and the samples of the REP series. The patterns revealed by those composites are essentially the same as that of the inorganic matrix, except for the peak positions in

the lower range of the 2θ angle ($4°–8°$) and the peak intensities. This lack of variation in the bulk diffractive features is strong evidence for the minor occurrence of delamination, and, hence, the overwhelming fraction of the MMT is believed to be intercalated with organic polymers. Furthermore, those intensive reflections of the composites compared to that of the pristine MMT at the $2\theta = 4°–8°$ range indicate also that the system is composed of alternating layers of polymer–MMT.[7]

On the other hand, the transfer of peak positions corresponding to d_{001} spacing toward to a lower 2θ angle can reasonably be attributed to the expansion of basal spacing of the composites. The average value of 1.52 nm in Table I is equivalent to Kojima et al.'s 1.51 nm,[8] being obtained from the nylon 6–clay hybrid, and comparable with 1.57 for the PMMA–clay[6] and 1.77 nm for the polyether–Na–MMT[9] hybrids. Accordingly, on the basis of this X-ray analysis, it can be concluded that the interlamellar distances can be increased with polymer loading by the emulsion technique without accompanying significant delamination.

In addition, the calculated value for the thickness of diglycidyl ether of bisphenol A by a chemical model was 0.52 nm, which corresponds to the average value of 0.57 nm of increased basal spacing. This means that a single layer of the polymer chain, on average, is confined between the clay gallery, being oriented parallel to the lateral direction of the interlayer. In view of this special limitation imposed on the polymer chains, the polymer molecules are expected to assume the type of planar conformation and their segmental motions are highly restricted.

SEM examination of the fracture surfaces in an extracted but uncured nanocomposite system containing 16.2% of the polymer reveals two different morphological phases, as are shown in Figure 4. The appearance of an irregular image in the figure (b) indicates that a delaminated nanocomposite can also be formed during the intercalation reaction, particularly when the polymer loading increases. However, judging from the XRD results, it seems reasonable that the significant fraction of the MMT was intercalated.

Molecular Characterization

The average molecular masses and polydispersity indices of polymers recovered from the composite extracts are summarized in Table II. All those
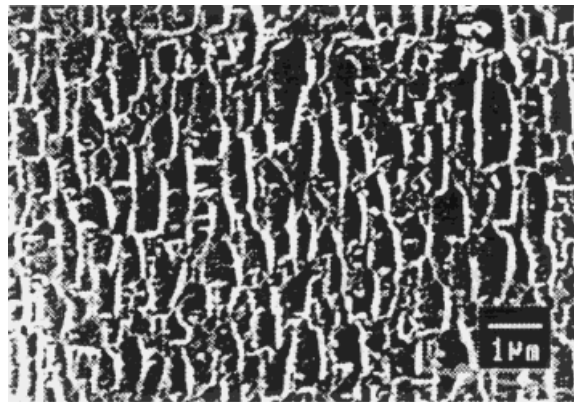
(a)
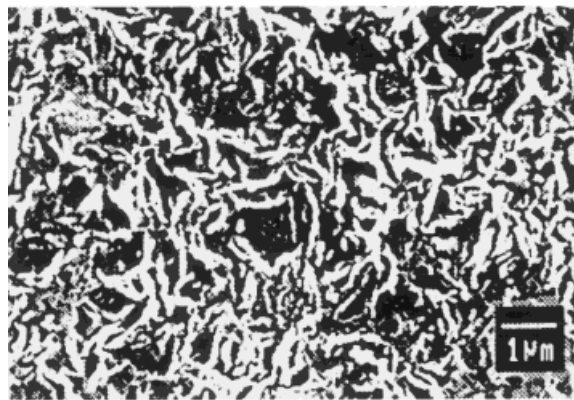
(b)

Figure 4 SEM of the extracted nanocomposite containing 16.2 wt % of the epoxy polymer.

$\bar{M}_w$'s exhibited by the composite extracts are in the order of 10^3 g/mol and are comparable with that of the epoxy polymer prepared with exclusion of MMT. This implies that the presence of MMT does not much influence the chain growth of the

Table II   Average Molecular Masses and Polydispersity Indices of Epoxy Homopolymer and Polymers Recovered from Acetone Extracts of the Nanocoposites by GPC

| Sample Code	$\overline{M_w}$ (g/mol)	Polydispersity Index ($\overline{M_w}/\overline{M_n}$)
Epoxy	1500	15.2
EXEP10	1700	24.5
EXEP20	1500	29.8
EXEP30	2200	22.1
EXEP40	2300	24.5
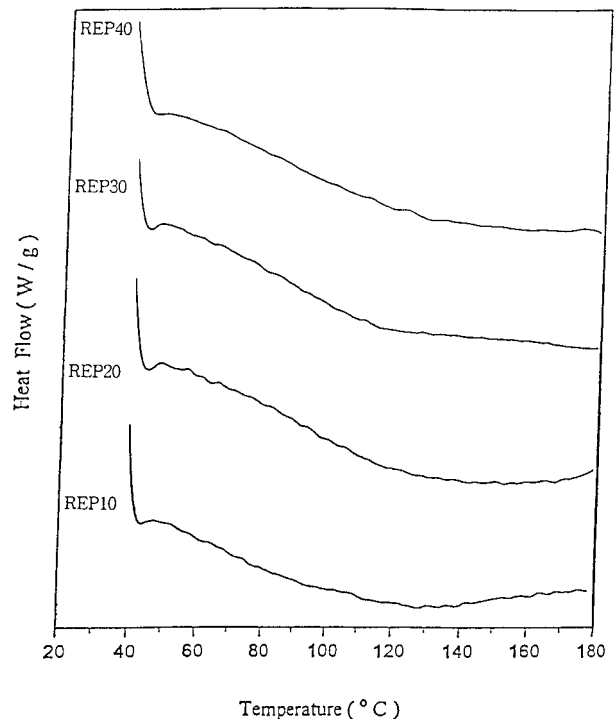
Figure 5 DSC thermograms of the extracted nanocomposites.

polymer molecules in the composites. Although the polydispersity variation shows no definite trend, the values of the composites appeared as slightly larger than that of neat epoxy, suggesting that the MMT can possibly affect the kinetics of the terminating step. On the basis of a reasonable assumption, on the other hand, that a swelled MMT can provide sites equally for the polymerization at both the inside and outside surfaces of the clay, the measured M_w's can be regarded as equivalent for both side polymers.

Thermal Characterization

DSC thermograms obtained from those extracted composites are illustrated in Figure 5, which reveal no evidence of thermal transition. The low molecular mass and polymer confinement are considered to be the most responsible. In contrast, the cured products show clear transition points corresponding approximately to the T_g of the cured epoxy polymer. Those endotherms in Figure 6 are referred most likely to the crosslinking of the epoxy resin loaded inside and outside the MMT particles. Moreover, the elevation of the transition temperatures with an increasing content of MMT
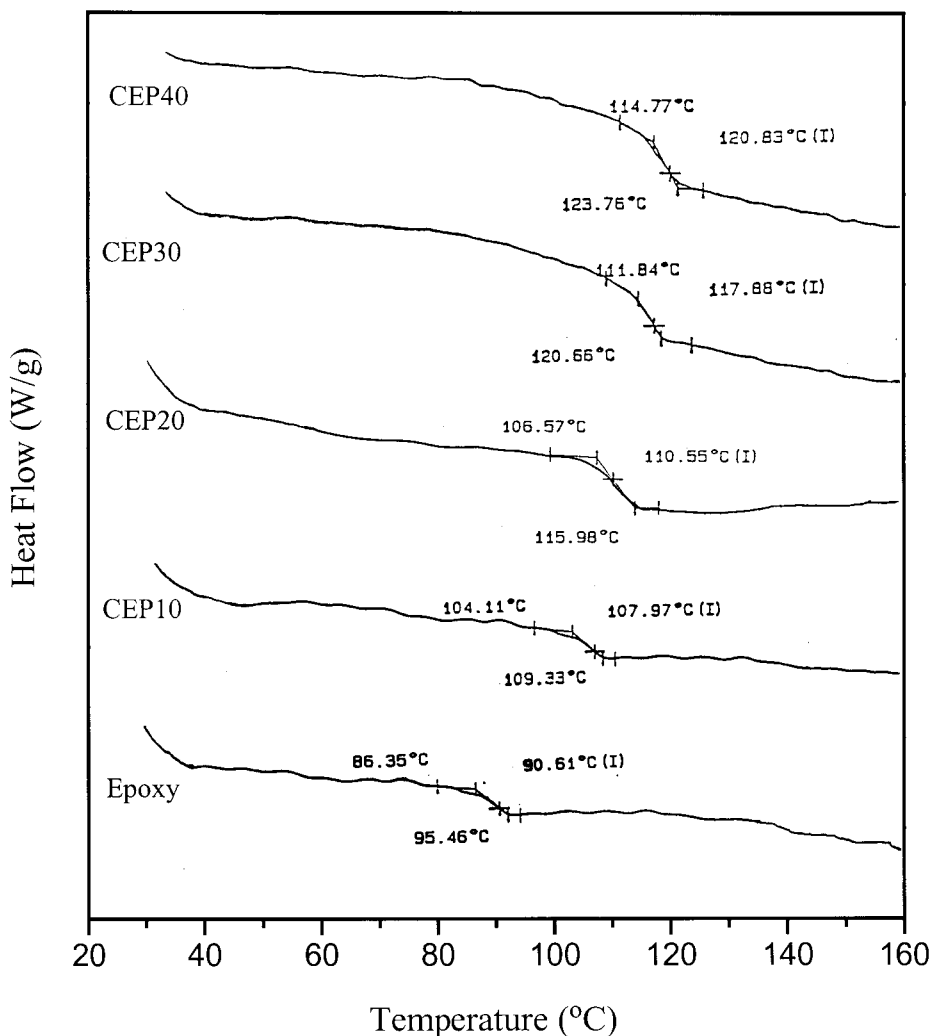
Figure 6   DSC thermograms of the cured epoxy polymer and the nanocomposites.

can easily be interpreted in terms of the heat-insulation effect of MMT, and this phenomenon is compatible with the results obtained from the following TGA experiments.

Figure 7 compares the TGA thermograms obtained from the cured products. Obviously, the onset temperatures of thermal decomposition shown by those composites are shifted significantly toward to the higher temperature range than that of pure epoxy polymer, indicating the enhancement of the thermal stability of the composites. It is also noticeable that the composites are showing nearly the same onset temperature range at around 280°C, regardless of their polymer contents. This is an indication that the heat-insulation effect of the inorganic host does not

depend much on the polymer contents of the composite, within the ranges of this study.

Physical Picture of Intercalation

On the basis of the swelling characteristics of clay in an aqueous system,[10,11] a quantitative description of the possibility of polymer intercalation by the emulsion technique can be made in terms of the swelled distance of the interlayer and the sizes of the monomer-containing micelles. The swelled distance of the clay interlayer can be predicted as follows:

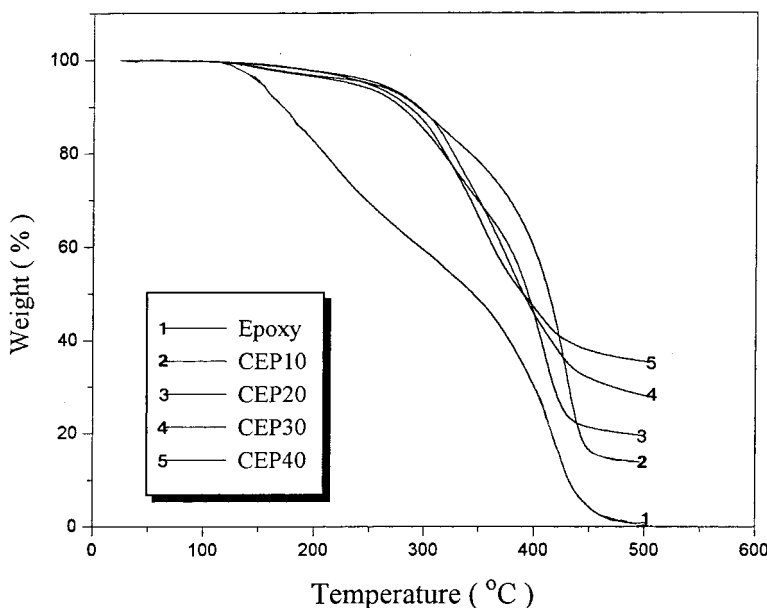$$d = [\varepsilon/100](t + R_{ion}) + R_{ion} \quad (\text{in m}),$$

Figure 7 TGA thermograms of the cured nanocomposites and the epoxy polymer.

where d is half the distance between the two layers; ε, the swelling volumetric strain (%); t, the thickness of the MMT mineral layer; and R_{ion}, the nonhydrated radius of typical ions that existed in the MMT interlayer. Fitting the parameters obtained from experiment, such as $\varepsilon = 500\%$, $t = 0.96$ nm, and $RNa^+ = 0.098$ nm,[11] to the above equation, the $2d$ value can be calculated as 35 nm when the MMT is assumed to be fully expanded.

On the other hand, the dimensions of monomer-containing micelles in a typical emulsion polymerization system are known to have values ranging from 2 to 10 nm.[12] This suggests that the swelled basal spacing of MMT in an aqueous system can provide enough space to penetrate those monomer-containing micelles and polymerization to occur, while those large-sized monomer droplets (10^3–10^4 nm) are simply adsorbed or bound to the outer surfaces of the MMT particles and polymerized.

of a condensation type of a polymer by emulsion polymerization with a small scale of concomitant delamination. The structural characterizations by FTIR and XRD for the extracted products give strong evidence that an overwhelming fraction of MMT is intercalated with the epoxy polymer. The enhanced thermal stability of those postcured products are corroborated by TGA and DSC analysis. The strong fixation of the polymer to the inorganic surfaces is believed to be due to the cooperative formation of the ion–dipole force acting between the polar functional groups of the polymer chain and the interlayer ions. The possibility of direct intercalation by this emulsion technique is proposed, demonstrating the quantitative relations of fully swelled distances of clay interlayers and the sizes of monomer-containing micelles.

CONCLUSIONS

Epoxy–MMT hybrid composites are successfully prepared by a simple technique of emulsion polymerization without using any kind of ion-exchange reaction with alkyl or aryl onium ions or by employing special coupling agents. The most striking result is the demonstration of direct intercalation

REFERENCES

1. E. Ruiz-Hitzky, *Mol. Cryst. Liq. Cryst.,* **161,** 433 (1988).
2. J. E. Mark, in *Hybrid Organic–Inorganic Composites,* ACS Symposium Series 585, American Chemical Society, Washington, DC, 1995.
3. P. Aranda and E. Ruizhitzky, *Acta Polym.,* **45,** 59 (1994).

4. P. B. Messersmith and E. P. Giannelis, *Chem. Mater.,* **6,** 1719 (1994).

5. A. Okada, A. Usuki, T. Kurauchi, and O. Kamigaito, in *Hybrid Organic–Inorganic Composites,* ACS Symposium Series 585, American Chemical Society, Washington, DC, 1995, Chap. 6, pp. 55.

6. D. C. Lee and L. W. Jang, *J. Appl. Polym. Sci.,* **61,** 1117 (1996).

7. S. D. Burnside and E. P. Giannelis, *Chem. Mater.,* **7,** 1597 (1995).

8. Y. Kojima, A. Usuki, M. Kawasumi, and A. Okada, *J. Polym. Sci. Part A,* **31,** 983 (1993).

9. J. Wu and M. M. Lerner, *Chem. Mater.,* **5,** 835 (1993).

10. H. Komine and N. Ogata, *Can. Geotech. J.,* **31,** 478 (1994).

11. H. Komine and N. Ogata, *Can. Geotech. J.,* **33,** 11 (1996).

12. G. Odian, *Principles of Polymerization,* 3rd ed., Wiley, New York, 1991.